Laser wakefield electron acceleration for γ-ray radiography application

Yuchi Wu (吴玉迟)*, Zongqing Zhao (赵宗清), Bin Zhu (朱 斌), Kegong Dong (董克攻), Xianlun Wen (温贤伦), Yingling He (何颖玲), Yuqiu Gu (谷渝秋), and Baohan Zhang (张保汉)

Science and Technology on Plasma Physics Laboratory, Research Center of Laser Fusion, China Academy of Engineering Physics, Mianyang 621900, China

**Corresponding author: wyc_one@sina.com*

Received November 9, 2011; accepted January 10, 2012; posted online March 15, 2012

An electron beam is obtained using laser wakefield electron accelerator, and converted into a γ-ray source after undergoing bremsstrahlung radiation in a dense material. A quasi-monoenergetic structure is observed when the length of the plasma channel was modified. The structure has a 58-MeV peak energy, 15-mrad (full-width at half-maximum) divergence angle, and 340-pC charge. The γ-ray source generated by this high-quality electron beam is brighter and has higher spatial and temporal resolutions than other conventional sources. A γ-ray radiography demonstrational experiment is performed. Pictures of a ball with different layers made of different materials are taken. The results show a clear structure and density resolution.

OCIS codes: 350.5400, 350.5720, 170.2670.
doi: 10.3788/COL201210.063501.

γ-ray radiography is widely used in nondestructive material testing or mechanical inspection[1]. The γ-ray source is usually produced using conventional accelerators with low electron energy and millimeter-scale beam focusing. With the rapid evolution of laser technology, the interaction of a high-intensity short laser pulse with underdense plasma produces large electric fields, which can be used to accelerate electrons. Accelerators have demonstrated accelerating electric fields of hundreds of gigavolts per meter[2−4], and electron bunches of several hundreds of mega electron volts to 1 GeV have been obtained[5−8]. These fields are thousands of times more intense than those achievable using conventional radio-frequency (RF) accelerators. Thus, laser accelerators have been considered as compact next-generation sources of energetic electrons and radiation[9,10]. The nonlinear behavior of the plasma wave drives the generation of energetic and low emanative electron beams[11]. The diameter and duration of the electron source are directly comparable with the laser focal spot size and laser pulse duration. Laser-plasma electron accelerators can be applied to generate a high-quality γ-ray source, which is obtained via the bremsstrahlung radiation of electrons slowing down in a conversion target with a high atomic number. Such gamma source has good brightness and higher spatial and temporal resolutions and has been produced in the experiments demonstrated in Refs. [12–14]. In this letter, we report a laser wakefield accelerator that generates an electron source for γ-ray radiography applications with low divergence and a large amount of charge.

The parameters of the electron source were estimated before the experiment. With the assumption that a 2π emissive γ-ray source produces a signal that can be recorded by a detector for dense matters, the source should achieve a 10^{10-11} photon yield and several mega electron volts of γ-ray photons. Monte Carlo (MC) simulations were performed using the MC Neutron and Photo Transport Code to evaluate the characteristics of the electron source. From the simulations, the electron energy should be up to several tens of mega electron volts. At this energy, the quantitative conversion efficiency of electrons to γ-ray photons in a high Z material is always above 25%. The γ-ray divergence angle is related to the electron beam quality, and a low emanative electron bunch induces a low emanative γ-ray source, which has been proved by both simulation and experiments[12−14]. Such an electron source is required for γ-ray radiography, with the energy level reaching several tens of mega electron volts and charge reaching at least 100 pC (10^{10} yield).

In the current experiment, a single laser pulse is used to trap and accelerate electrons. The physics of this process is highly nonlinear and can be explained using the "bubble" regime[15−17]. The nonlinear evolution of the laser pulse via self-focusing[18] and self-compression[19] leads to an increase in the laser intensity and the formation of an electron-evacuated cavity (the bubble) filled with ions and surrounded by a dense wall of electrons. When the electron density at the walls reaches a threshold value, self-injection occurs at the back of the bubble. The injection stops when the charge density of the trapped bunch becomes comparable with the charge density at the bubble walls. This short and localized injection forms a quasi-monoenergetic electron bunch. The occurrence of a continuous self-focusing phenomenon is a precondition for obtaining a quasi-monoenergetic electron bunch.

The experiment was performed on a Ti:sapphire laser. The laser was the SILEX–I Ti:sapphire laser system[20] based on the chirped-pulse amplification technique, which operates at a center wavelength of 800 nm and delivers 30-fs (full-width at half-maximum (FWHM)) pulses with on-target energies of 7 J. The experimental setup is shown in Fig. 1. The laser beam is focused using an $f/8.7$ off-axis parabolic mirror on the front edge of a supersonic helium gas jet boundary at a height of 2 mm. The waist width of the focal spot is 13 μm. In the experiment, two types of nozzles were used. One is a 10-mm-long supersonic slit nozzle, and the other is a 2.7-

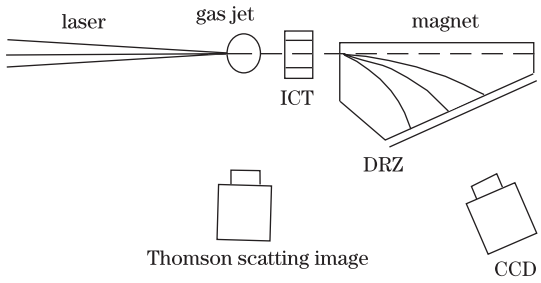

Fig. 1. Schematic of the experimental arrangement.

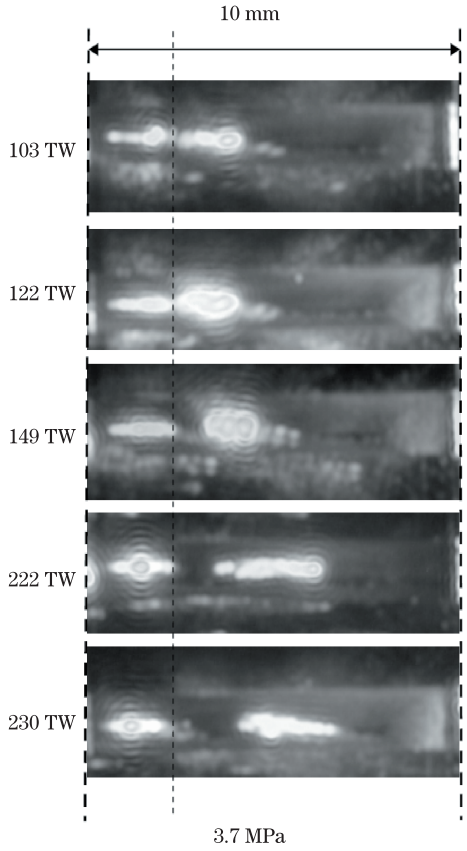

Fig. 2. Thomson scattering image with different laser intensities at a gas jet backing pressure of 3.7 MPa. The total length of the laser propagation increases with laser power. Two thick dashed lines denote the boundary of the 10-mm-long slit nozzle. The laser crosses the gas jet from left to right. The thin dashed line shows the first part of the self-focusing laser, which has a constant length of approximately 2 mm.

mm-diameter supersonic conic nozzle. The gas densities of these two nozzles were measured using an interferometer before the experiments[21]. The densities can be controlled from 5×10^{18} to 5×10^{19} cm^{-3} by changing the backing pressure.

After the laser plasma interaction, the charge per bunch was measured using an integrating current transformer (ICT) set in the laser axis behind the gas jet. A 2-mm-thick polyethylene filter was set at the front of the ICT to eliminate electron bunches below 1 MeV. The energy spectra of the electron bunches ejected from the gas jet were measured using a diagonal radioactive zone (DRZ) phosphor screen and a permanent magnet. The permanent magnet can disperse the electrons according to their different kinetic energies at different positions on the DRZ screen. The scintillating image on the DRZ was recorded using a charge-coupled device (CCD) camera. Another CCD was oriented perpendicular to the laser polarization to measure the Thomson scattering of the laser pulse.

In the experiment, the 10-mm-long slit nozzle was adopted to obtain a long and continuous plasma acceleration channel, which can accelerate electrons to high energies. The Thomson scattering image is shown in Fig. 2, with the gas jet backing pressure maintained at 3.7 MPa, providing an initial plasma electron density n_e of 8×10^{18} cm^{-3}. Unfortunately, the self-focusing in the laser transmission was discontinuous. Although the total length increases with the laser intensity, the self-focusing channel was divided into two parts. The first part always has a length of 2 mm, and the second part lengthens with laser intensity. The distance between the two parts also increases. The typical electron energy spectrum is shown in Fig. 3. The energy of the electron bunch represents a continuous spectrum extending to more than 100 MeV with a peak of 34 MeV. The bunch divergence angle is approximately 110 mrad. Such electron bunches are not fit for γ-ray radiography applications.

A three-dimensional (3D) nonlinear phenomenological theory indicated that the laser depletion and wakefield dephasing lengths should match to achieve the ideal laser wakefield acceleration (LWFA)[16]. When the depletion length is longer than the dephasing length, the electrons will dephase in wakefield and degenerate in quality. When the depletion length is less than the dephasing length, the electrons cannot reach optimum energy and beam quality. The laser depletion length indicates a self-guided propagation of the laser beam without significant variations of the pulse profile over the interaction distance[16]. The self-focusing length can be used to estimate this length. Thus, in the current experiment, a discontinuous self-focusing channel also leads to an unsta-

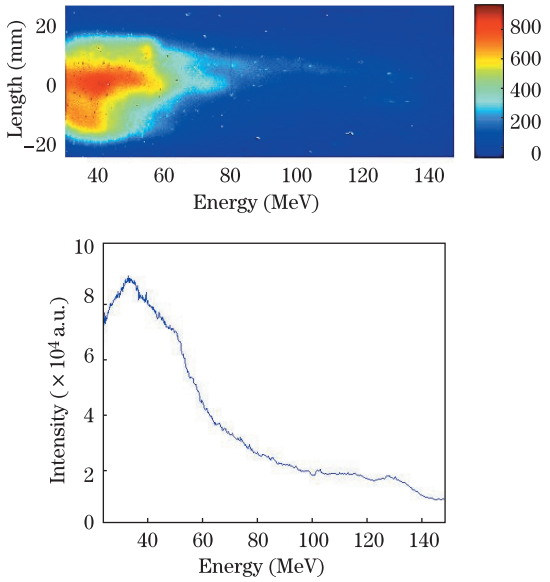

Fig. 3. Typical electron energy spectrum in the experiment which uses a 10-mm-long slit nozzle.

ble acceleration process in which the electron would undergo a complex and unstable acceleration–deceleration–reacceleration process. Hence, a quasi-monoenergetic electron bunch cannot be obtained, and the electron beam generated in such process will be of bad quality. The first part of the self-focusing channel in the acceleration experiment using the 10-mm-long nozzle maintains a length of 2 mm, indicating a steady process in this part. If only this self-focusing length is used to perform the experiment, a quasi-monoenergetic electron bunch may be obtained from this part. Therefore, the experiment was conducted using the 2.7-mm-diameter nozzle to meet the theoretical matching condition[15−17]. A backing pressure of 2.5 MPa was chosen to provide an initial plasma electron density n_e of 2.3×10^{19} cm^{-3}, and the laser power was maintained at approximately 70 TW, corresponding to a normalized laser vector potential $a_0 = 8.5\times10^{-10}\lambda_0 I_0^{1/2} = 2.2$. According to the Thomson scattering image in Fig. 4, the self-focusing channel is continuous, providing the precondition for acceleration. The electron energy spectrum corresponding to Fig. 4 is shown in Fig. 5. A quasi-monoenergetic electron bunch with a peak energy of 58 MeV and energy spread of $\triangle E/E$=15% was observed. The divergence angle of the quasi-monoenergetic structure is 15 mrad (FWHM). The electron bunch has a 340-pC charge, as measured by the ICT. All of the necessary factors are satisfied for the γ-ray radiography application. The result is detailed in Ref. [22].

After the optimization of the electron bunch, an experiment demonstrating γ-ray radiography was performed. The experimental setup is shown in Fig. 6. An electron beam was generated via laser–plasma interaction. Then, the electron bunch was converted into a γ-ray inside a 2-mm-thick tantalum converter placed 2 mm from the center of the nozzle. A magnet was set behind the converter to deflect the residuary electron and hence avoid the bremsstrahlung radiation of the electrons inside the object. A layered ball was located 150-mm away from the gas jet as the radiographic object. The ball is composed of a 1.8-mm-thick plastic outer layer, a 1.8-mm-thick aluminum middle layer, and a copper ball at the core with a total diameter of 10 mm. The γ-ray image was recorded using a phosphor screen imaged on a CCD camera. The distance between the object and the phosphor screen is 150 mm. A photographic lens was mounted on the camera with a focal length of 50 mm and an F number of $f/1.4$.

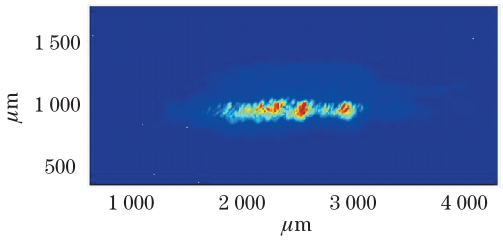

Fig. 4. Thomson scattering image in the experiment which uses a 2.7-mm-diameter nozzle. The backing pressure is 2.5 MPa, and the laser power is maintained at 70 TW. The laser shows a continuous full-range transport of the nozzle, with a length about 2 mm corresponding to the first part of the slit nozzle. The laser crosses the gas jet from left to right.

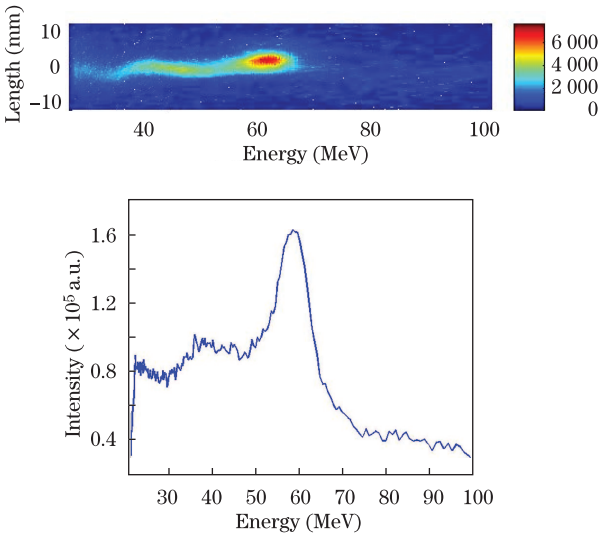

Fig. 5. Quasi-monoenergetic electron energy spectrum.

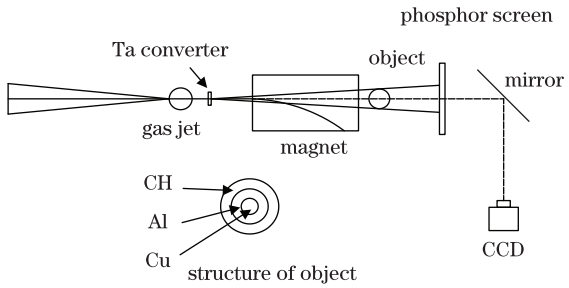

Fig. 6. Schematic of the γ-ray radiography demonstrational experiment and structure of the object.

The result of the γ-ray radiographic experiment is shown in Fig. 7. The experimental image shows the layered structure. The three different colors indicate the three layers of the object. The differences in color correspond to the different γ-ray transmissions determined by the density and atomic number of the material. The low density and atomic number lead to a higher transmission. In Fig. 7, higher counts can be seen at the outside of the ball, which then decline from the surface to the core. The transmission contains some density information, which can be used to calculate the density of the object. From the boundary between two different layers, the size of the γ-ray source and special resolution can be calculated using some mathematical processes, such as Abel inversion, among others. A detailed analysis of this radiograph will be presented in future work.

In conclusion, an electron source for γ-ray radiography obtained using a laser wakefield electron accelerator is demonstrated. The electron source produces the γ-ray source via bremsstrahlung radiation inside a high Z converter, and its parameters are calculated using a MC simulation. A quasi-monoenergetic electron bunch was obtained in the laser wakefield accelerator by modifying the acceleration length. The electron bunch has a 58-MeV peak energy, 15-mrad (FWHM) divergence angle,

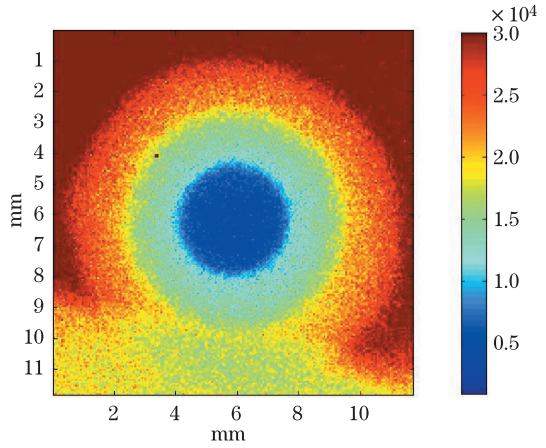

Fig. 7. Radiographic image of a 1-cm-diameter globose object with a layered structure. The three circles with different colors show the three layers composed of different materials. The colors also indicate the γ-ray transmissions, which can be used to analyze the material of each layer.

and 340-pC electron energy charge. The γ-ray radiography demonstrational experiments are performed using this electron source. The γ-ray image clearly shows a complex object, implying that the electron source has excellent performance and good application potential.

Such electron source can produce a high-energy γ-ray photon source with sufficient brightness and low divergence. The photon source is also expected to be ultrashort because the electron source duration is comparable with the laser pulse duration (30 fs). Ultrashort γ-ray sources are promising for several applications, including fast moving object monitoring or high-density metal compression visualization[1]. These electrons and γ-ray sources are brighter and have higher spatial and temporal resolutions than conventional sources. All of these excellent characteristics, combined with the decreasing cost and size of terawatt lasers, make such sources extremely useful for radiographic applications. γ-ray radiography demonstrational experiments will be performed in future studies.

This work was supported by the China Acdamy of Engineering Physics Project (No. 2006Z0202), the State Key Program of the National Natural Science of China (No. 10535030), and the National Natural Science Foundation of China (No. 10975121).

References

1. Y. J. Chen, L. R. Bertolini, G. J. Caporaso, F. W. Chambers, E. G. Cook, S. Falabella, F. J. Goldin, G. Guethlein, D. D. M. Ho, J. F. McCarrick, S. D. Nelson, R. Neurath, A. C. Paul, P. A. Pincosy, B. R. Poole, R. A. Richardson, S. Sampayan, S. Sampayan, L. F. Wang, J. A. Watson, G. A. Westenskow, and J. T. Weir, in *Proceedings of 21st International Linear Accelerator Conference, Gyeongju, Sorea* (2002).
2. A. Modena, Z. Najmudin, A. E. Dangor, C. E. Clayton, K. A. Marsh, C. Joshi, V. Malka, C. B. Darrow, C. Danson, D. Neely, and F. N. Walsh, Nature **377,** 606 (1995).
3. V. Malka, S. Fritzler, E. Lefebvre, M.-M. Aleonard, F. Burgy, J.-P. Chambaret, J.-F. Chemin, K. Krushelnick, G. Malka, S. P. D. Mangles, Z. Najmudin, M. Pittman, J.-P. Rousseau, J.-N. Scheurer, B. Walton, and A. E. Dangor, Science **298,** 1596 (2002).
4. W. P. Leemans, P. Catravas, E. Esarey, C. G. R. Geddes, C. Toth, R. Trines, C. B. Schroeder, B. A. Shadwick, J. van Tilborg, and J. Faure, Phys. Rev. Lett. **89,** 174802 (2002).
5. J. Faure, Y. Glinec, A. Pukhov, S. Kiselev, S. Gordienko, E. Lefebvre, J.-P. Rousseau, F. Burgy, and V. Malka, Nature **431,** 541 (2004).
6. C. G. R. Geddes, Cs. Toth, J. van Tilborg, E. Esarey, C. B. Schroeder, D. Bruhwiler, C. Nieter, J. Cary, and W. P. Leemans, Nature **431,** 538 (2004)
7. S. P. D. Mangles, C. D. Murphy, Z. Najmudin, A. G. R. Thomas, J. L. Collier, A. E. Dangor, E. J. Divall, P. S. Foster, J. G. Gallacher, C. J. Hooker, D. A. Jaroszynski, A. J. Langley, W. B. Mori, P. A. Norreys, F. S. Tsung, R. Viskup, B. R. Walton, and K. Krushelnick, Nature **431,** 535 (2004).
8. J. S. Liu, C. Q. Xia, W. T. Wang, H. Y. Lu, Ch. Wang, A. H. Deng, W. T. Li, H. Zhang, X. Y. Liang, Y. X. Leng, X. M. Lu, C. Wang, J. Z. Wang, K. Nakajima, R. X. Li, and Z. Z. Xu, Phys. Rev. Lett. **107,** 035011 (2011).
9. T. Tajima and J. M. Dawson, Phys. Rev. Lett. **43,** 267 (1979).
10. E. Esarey, P. Sprangle, J. Krall, and A. Ting, IEEE Trans. Plasma Sci. **24,** 252 (1996).
11. S. Fritzler, E. Lefebvre, V. Malka, F. Burgy, A. E. Dangor, K. Krushelnick, S. P. D. Mangles, Z. Najmudin, J.-P. Rousseau, and B. Walton, Phys. Rev. Lett. **92,** 165006 (2002).
12. R. D. Edwards, M. A. Sinclair, T. J. Goldsack, K. Krushelnick, F. N. Beg, E. L. Clark, A. E. Dangor, Z. Najmudin, M. Tatarakis, B. Walton, M. Zepf, K. W. D. Ledingham, I. Spencer, P. A. Norreys, R. J. Clarke, R. Kodama, Y. Toyama, and M. Tampo, Appl. Phys. Lett. **80,** 2129 (2002).
13. Y. Glinec, J. Faure, L. Le Dain, S. Darbon, T. Hosokai, J. J. Santos, E. Lefebvre, J. P. Rousseau, F. Burgy, B. Mercier, and V. Malka, Phys. Rev. Lett. **94,** 025003 (2005).
14. A. Ben-Ismaı, O. Lundh, C. Rechatin, J. K. Lim, J. Faure, S. Corde, and V. Malka, Appl. Phys. Lett. **98,** 264101 (2011).
15. A. Pukhov and J. Meyer-ter-Vehn, Appl. Phys. B **74,** 355 (2002).
16. W. Lu, C. Huang, M. Zhou, M. Tzoufras, F. S. Tsung, W. B. Mori, and T. Katsouleas, Phys. Plasmas **13,** 056709 (2006).
17. W. Lu, C. Huang, M. Zhou, W. B. Mori, and T. Katsouleas, Phys. Rev. Lett. **96,** 165002 (2006).
18. G. Z. Sun, E. Ott, Y. C. Lee, and P. Guzdar, Phys. Fluids **30,** 526 (1987).
19. J. Faure, Y. Glinec, J. J. Santos, F. Ewald, J.-P. Rousseau, S. Kiselev, A. Pukhov, T. Hosokai, and V. Malka, Phys. Rev. Lett. **95,** 205003 (2005).
20. H. S. Peng, X. J. Huang, Q. H. Zhu, X. D. Wang, K. N. Zhou, X. F. Wei, X. M. Zeng, L. Q. Liu, X. Wang, Y. Guo, D. H. Lin, B. Xu, L. B. Xu, X. L. Chu, and X. M. Zhang, Laser Physics **16,** 244 (2006).
21. Y. C. Wu, L. Wang, H. B. Wang, H. J. Liu, F. F. Ge, J. B. Chen, Z. J. Zheng, B. H. Zhang, Y. Q. Gu, and C. W. Yang, High Power Laser and Particle Beams (in Chinese) **19,** 1129 (2007).
22. K. G. Dong, Y. Q. Gu, Y. C. Wu, B. Zhu, L. F. Cao, Y. L. He, H. J. Liu, W. Hong, W. M. Zhou, Z. Q. Zhao, C. Y. Jiao, X. L. Wen, B. H. Zhang, and X. F. Wang, Acta. Phys. Sin. (in Chinese) **59,** 8733 (2010).